Molecular Pharmacology Fast Forward. Published on May 30, 2020 as DOI: 10.1124/mol.119.118786
This article has not been copyedited and formatted. The final version may differ from this version.

A Methyl Scan of the Pyrrolidinium Ring of Nicotine Reveals Significant Differences in its Interactions with α7 and α4β2 Nicotinic Acetylcholine Receptors

Hong Xing, Kristin W. Andrud, Ferenc Soti, Anne Rouchaud, Stephan C. Jahn, Ziang Lu, Yeh-Hyon Cho, Sophia Habibi, Patrick Corsino, Svetoslav Slavov, James R. Rocca, Jon M. Lindstrom, Ron J. Lukas and William R. Kem*

Department of Pharmacology and Therapeutics, College of Medicine, University of Florida, Gainesville, FL 32610, USA (HX, KWA, FS, AR, SH, SJ, LZ, Y-HC, PC, WRK); National Center for Toxicological Research, US Food and Drug Administration, Jefferson, AR 72079 (SS); AMRIS, McKnight Brain Institute, University of Florida, (JRR); Department of Neuroscience, University of Pennsylvania, Philadelphia, PA 19104 (JML); Division of Neurobiology, Barrow Neurological Institute, Phoenix, AZ 85013 (RJL); Present Address: Dept. of Biological Sciences, University of Denver, Denver, CO 80208 (KWA)

Molecular Pharmacology Fast Forward. Published on May 30, 2020 as DOI: 10.1124/mol.119.118786
This article has not been copyedited and formatted. The final version may differ from this version.

Disclaimer: The views presented in this article are those of the authors and do not necessarily reflect those of the U.S. Food and Drug Administration. No official endorsement is intended nor should be inferred.

Key Words: Acetylcholine, Drug Design, Methyl Scan, Neurodegenerative Disease, Nicotine, Nicotinic Acetylcholine Receptor, Schizophrenia, Smoking Cessation

Molecular Pharmacology Fast Forward. Published on May 30, 2020 as DOI: 10.1124/mol.119.118786
This article has not been copyedited and formatted. The final version may differ from this version.

Running title: Methyl scan of the nicotine pyrrolidinium ring

*To Whom Correspondence Should Be Addressed

Name: William R. Kem

Phone: 352-392-0669

FAX: 352-392-9696

Email: **wrkem@ufl.edu**

Address: Department of Pharmacology and Therapeutics

University of Florida

P.O. Box 100267

Gainesville, FL 32610-0267

Number of text pages: 32

Number of tables: 6

Number of figures: 4

Number of references: 61

Number of words in Abstract: 232

Number of words in Introduction: 935

Number of words in Discussion: 1791

Abbreviations: AChBP, acetylcholine binding protein; α-BTX, α-bungarotoxin; nAChR, nicotinic acetylcholine receptor

Molecular Pharmacology Fast Forward. Published on May 30, 2020 as DOI: 10.1124/mol.119.118786
This article has not been copyedited and formatted. The final version may differ from this version.

ABSTRACT

The two major nicotinic acetylcholine receptors (nAChRs) in the brain are the α4β2 and α7 subtypes. A "methyl scan" of the pyrrolidinium ring was used to detect differences in nicotine's interactions with these two receptors. Each methylnicotine was investigated using voltage-clamp and radioligand binding techniques. Methylation at each ring carbon elicited unique changes in nicotine's receptor interactions. Replacing the 1'-N methyl with an ethyl group or adding a second 1'-N methyl group significantly reduced interaction with α4β2 but not α7 receptors. 2'-methylation uniquely enhanced binding and agonist potency at α7 receptors. Although 3'and 5'trans-methylations were much better tolerated by α7 receptors than α4β2 receptors, 4' methylation decreased potency and efficacy at α7 receptors much more than at α4β2 receptors. While cis-5'-methylnicotine lacked agonist activity and displayed a low affinity at both receptors, trans-5'methylnicotine retained considerable α7 receptor activity. Differences between the two 5'-methylated analogs of the potent pyridyl oxymethylene-bridged nicotine analog A84543 were consistent with what was found for the 5'-methylnicotines. Computer docking of the methylnicotines to the *Lymnaea* AChBP crystal structure containing two persistent waters predicted most of the changes in receptor affinity that were observed with methylation, particularly the lower affinities of the cis-methylnicotines. The much smaller effects of 1'-, 3'- and 5'-methylations and the greater effects of 2'- and 4'-methylations on nicotine α7 nAChR interaction might be exploited for the design of new drugs based on the nicotine scaffold.

Molecular Pharmacology Fast Forward. Published on May 30, 2020 as DOI: 10.1124/mol.119.118786
This article has not been copyedited and formatted. The final version may differ from this version.

SIGNIFICANCE

Using a comprehensive "methyl scan" approach we show that the orthosteric binding sites for acetylcholine and nicotine in the two major brain nicotinic acetylcholine receptors interact differently with the pyrrolidinium ring of nicotine, and suggest reasons for the higher affinity of nicotine for the heteromeric receptor. Potential sites for nicotine structure modification were identified that may be useful in the design of new drugs targeting these receptors.

Molecular Pharmacology Fast Forward. Published on May 30, 2020 as DOI: 10.1124/mol.119.118786
This article has not been copyedited and formatted. The final version may differ from this version.

INTRODUCTION

Nicotine activates a variety of ligand-gated acetylcholine receptors (nAChRs) that play important signaling roles in neuronal and some non-neuronal cells and has a number of potentially therapeutic effects. However, it is one of the most addictive of drugs when self-administered as a tobacco product. Nicotine is also a widely used as a useful smoking cessation drug in non-smoked formulations (Prochaska and Benowitz, 2016). Several nicotine analogs have already been tested as potential treatments for neurodegenerative and psychiatric disorders.

Vertebrate nAChRs are cation permeant ion channels composed of five homologous subunits. Molecular biological investigations have revealed genes for 17 different subunits, so a large number of subunit combinations is theoretically possible and >15 pentameric subunit combinations have already been identified in mammalian tissues (Wu and Lukas, 2011). At least two α subunits occur in each nAChR pentamer. Agonist binding sites are located within a groove between the N-terminal extracellular domains of an α subunit and an adjacent subunit. The α7 and α4β2 nAChRs are the most numerous and widely distributed receptor subtypes in the brain and have been demonstrated to participate in cognitive function. α7 nAChRs are mainly homomeric complexes containing five α7 monomers, though small concentrations of α7β2 nAChRs also occur in the brain (Moretti et al., 2014). All the other nAChRs contain two or three non-α subunits. Significant decreases in the concentrations of these two receptors have been found in the postmortem brains of Alzheimer's and Parkinson's disease patients (Burghaus et al., 2003). In many schizophrenics, the alpha7 receptor is expressed at lower than normal levels and this is thought to contribute to deficient sensory gating and cognition (Martin et al., 2004). There is considerable pharmaceutical interest in developing selective nicotinic agonists and allosteric modulators that target either α7 or α4β2 nAChRs for treating cognitive deficits in

Molecular Pharmacology Fast Forward. Published on May 30, 2020 as DOI: 10.1124/mol.119.118786
This article has not been copyedited and formatted. The final version may differ from this version.

neurodegenerative diseases. Partial agonists for α4β2 receptors like varenicline and cytisine are widely used as smoking cessation drugs. In addition, α7 nAChRs occuring in macrophages (and their brain counterparts, microglia), lymphocytes, keratinocytes, lung epithelium and certain cancer cells modulate a variety of signaling pathways and have become attractive therapeutic targets (Bertrand et al., 2015; Bouzat et al, 2018).

Despite the widespread use of nicotine as an experimental nAChR probe and lead compound for the design of new drugs, the molecular basis for its preferential interactions with certain nAChRs is still poorly understood. Initial chemical modification and mutagenesis studies led to the identification of key aromatic amino acid side chains and peptide bonds constituting ACh binding sites (Changeux, 2012). A combination of cation-pi, electrostatic, hydrogen and van der Waals bonding forces are involved in ligand (agonist and competitive antagonist) recognition (Cashin et al., 2005; Xiu et al., 2009; Puskar et al., 2011). High resolution crystal structures of several homologous acetylcholine binding proteins (AChBPs) and their analogs mutated to better resemble the α7 orthosteric binding site have been available for some time (Celie et al., 2004; Hansen et al., 2005; Li et al., 2011). Crystal structures of the extracellular portions of the adult skeletal muscle α1 subunit and the α10 subunit binding α-bungarotoxin (α-BTX) have been reported (Delissanti et al., 2007; Zouridakis et al., 2014). Recently, a crystal structure of the nearly whole $\alpha4_2\beta2_3$ nAChR became available (Morales-Perez et al, 2016). These structures have been very useful for developing homology models of various nAChRs and have enabled ligand docking studies.

In view of the multiplicity of nAChRs and the need to minimize the adverse effects of nicotinic drugs on unintended nAChRs, it is desirable to identify structural differences between their orthosteric binding sites to enable the design of subtype selective drugs. In the present study

Molecular Pharmacology Fast Forward. Published on May 30, 2020 as DOI: 10.1124/mol.119.118786
This article has not been copyedited and formatted. The final version may differ from this version.

we employ a "methyl scan" (Black et al., 1972) approach to assess the consequences of single methyl substitutions for each of the eight hydrogens located on the pyrrolidinium ring of nicotine. Methyl substitution was selected because of its relatively minimal effect (a 16 % increase) in the mass of the pyrrolidinium moiety. The methyl group, like the four methylene groups in this ring, does not appreciably affect the lipophilic nature of the ring, introduces no new hydrogen-bonding atoms and does not diminish ionization of the pyrrolidinium nitrogen, which has been shown to be essential for efficient nAChR binding by this compound (Barlow and Hamilton, 1962; Jeng and Cohen, 1980).

The actions of a few alkylated nicotines on isolated tissues and organs have been reported (Glassco et al., 1994; Dukat et al., 1996). Two laboratories reported extensive rat brain nAChR (later shown to be largely α42β) binding data on the effect of individual methyl substitutions at 4 of the 8 hydrogens on the pyrrolidinium ring (Lin *et al*. 1994; Kim *et al*. 1996; Wang et al., 1998). In this paper we report a comprehensive functional and radioligand binding analysis of all the possible chiral nicotine analogs generated by methyl replacement of each H atom attached to the pyrrolidinium ring of (S)nicotine for α7 as well as α4β2 nAChRs. In addition, we evaluate the effect of increasing the size of the pre-existing 1'N-methyl group. To test the generality of our results with nicotine, we extended part of our methyl-scan to a highly potent nicotine analog, A84543, whose two nicotine-like rings are connected through an oxymethylene bridge that preserves the chirality of the 2'-pyrrolidinium ring (Abreo et al., 1996). Our results indicate that the pyrrolidinium moiety in these compounds has a similar binding mode in both nAChR binding sites but that the α7 site is less sensitive to most methyl substitutions.

[Fig. 1]

Molecular Pharmacology Fast Forward. Published on May 30, 2020 as DOI: 10.1124/mol.119.118786
This article has not been copyedited and formatted. The final version may differ from this version.

MATERIALS AND METHODS

Nicotine analogs

Preparation of all known compounds followed methods already described in the literature (See Fig. 1 in Rouchaud and Kem (2012) for a summary of most methods we employed). The compound ^{1}H and ^{13}C NMR spectral and MS spectrometric data of compounds whose syntheses were previously reported agreed with the published data. The chiral HPLC conditions for obtaining the individual enantiomers from the racemic 2'-, 3'- and 5'methylnicotines are provided in the Supplement. Nicotine dihydrogen tartrate salt (MW 462) was obtained from Sigma-Aldrich (St. Louis, MO). 1'-Methylnicotinium iodide (MW 304) was purchased from Toronto Research Chemicals (Toronto, Canada) and its identity was checked by NMR spectroscopy. In this paper the relative configurations (cis- or trans-) of the pyrrolidinium ring methyl substituents are always expressed with respect to the configuration of the pyridyl substituent. All alkylnicotines in Tables 1-5 have the same 2'(S)-pyrrolidinium ring configuration as in natural (S)nicotine. Data for 3'-methyl and 5'-methyl(R)nicotines are presented in Table 6.

Functional experiments with *Xenopus* oocytes

Frogs were purchased, maintained and used under a UF IACUC approval for the Kem laboratory. Mature female frogs (*Xenopus laevis*) were anesthetized by immersion in a 1.5 g/L solution of ethyl 3-aminobenzoate methanesulfonate (MP Biomedicals, Solon, OH) for 30 min. After the frog was completely unresponsive and immobile it was decapitated with a guillotine and its spinal cord pithed before excision of the ovary, which was placed into calcium-free Barth saline (88 mM NaCl, 1 mM KCl, 2.38 mM $NaHCO_3$, 0.82 mM $MgSO_4$, 15 mM HEPES, 0.012

Molecular Pharmacology Fast Forward. Published on May 30, 2020 as DOI: 10.1124/mol.119.118786
This article has not been copyedited and formatted. The final version may differ from this version.

mg/ml tetracycline hydrochloride (Sigma-Aldrich), pH 7.3±0.1), opened with forceps and washed three times with saline. Then 50 ml of 1.25 mg/ml type 1 collagenase (Worthington Biochemical Corporation, Freehold, NJ) solution dissolved in Ca^{2+}-free Barth saline was added and the oocyte containing mass was gently shaken for 2 hours at room temperature. After washing three times with calcium-free saline and then three times with Barth saline containing 0.7 mM Ca^{2+}, healthy stage 5 oocytes were transferred into dishes and incubated at 17°C overnight. Oocytes were routinely injected with 50 nl of a solution containing 20 ng α7 mRNA or 50 nl of a mixture of α4 and β2 mRNA (10 ng each), using a Drummond Nanoject II Auto-Injector. In some pilot experiments, oocytes were injected with 4:1 or 1:4 ratios (20 ng mRNA, total) of the two mRNAs to determine whether nicotine action under our experimental conditions was sensitive to subunit stoichiometry (Nelson et al., 2003**).** Finally, in one final set of experiments intended to investigate only the high agonist sensitivity $\alpha4_2\beta2_3$ nAChR, an equal weight (5ng) of RNA for the human β2AGSα4 concatamer was injected with 5 ng β2 RNA in each oocyte, since this ratio has been shown to minimize expression of alternative stoichometries of this receptor (Kuryatov et al., 2005;2007). Injected oocytes were cultured in Barth's saline for 5-10 days at 17°C with daily changes in the saline prior to recordings.

Individual oocytes were placed into a 20 µl oocyte perfusion chamber (Model OPC-1 connected to a ValveLink8.2 system, Automate Scientific, Berkeley, CA) and perfused at a rate of 2.0 ml/min at room temperature with frog Ringer's solution (115 mM NaCl, 2.5 mM KCl, 10 mM HEPES, 1.8 mM $CaCl_2$, pH 7.3) containing 1 µM atropine sulfate (Sigma-Aldrich) to block potential muscarinic responses. The two-microelectrode voltage-clamp technique was used to measure current responses at a constant holding potential (-60 mV for α7 and -50 mV for α4β2 nAChRs). The voltage-measuring microelectrode (filled with 3M KCl solution) resistance was

Molecular Pharmacology Fast Forward. Published on May 30, 2020 as DOI: 10.1124/mol.119.118786
This article has not been copyedited and formatted. The final version may differ from this version.

0.5-3.0 MΩ and the current-passing electrode (containing 250 mM CsCl and 100 μM EGTA) resistance was 0.5-2.0 MΩ. Membrane currents were recorded with an AxoClamp-2 (Axon Instruments, Union City, CA). Sampling rates were between 5 and 10 Hz. Compounds were transiently applied (2 sec for α7 and 5 sec for α4β2 receptors) to avoid a cumulative desensitization. A rapid flow rate (2.0 ml/sec) permitted complete replacement of the fluid bathing the oocyte at approximately 3X per second. Initially each oocyte received two control applications of a near maximal stimulatory concentration of ACh (1 mM ACh for α7 and 100 μM ACh for α4β2 receptors) to obtain a consistent response. ACh control applications alternated with test compound applications every 5 min. The peak current response for a given compound concentration was then normalized with respect to the mean current response obtained by averaging the responses for the ACh applications before and after that test concentration. Clampfit 8.1 (Axon Instruments) was used for data acquisition and Prism 3.0 (GraphPad, San Diego, CA, USA) for analysis. The concentration-response curve for each compound was calculated by fitting the data using a modified Hill equation:

$$\text{Response I} = I_{max}\,(\text{Agonist}) / [(\text{Agonist})^{n}+(EC_{50})^{n}]$$

where each Response current I is normalized with respect to the above-mentioned mean ACh control response and I_{max} denotes the maximal response current for the agonist, again relative to the ACh control response, and n is the Hill slope. It has been demonstrated that α7 nAChR total current (net charge over time)-concentration response curves are shifted to lower concentrations relative to transient peak response-concentration curves (Papke and Thinschmidt, 1998). Thus, we measured net charge as well as peak current responses for each oocyte response. Total current over a 20 s interval (including the 2 s drug application period) was measured and the net charge response was obtained after subtraction of baseline current for the same 20 s period.

Molecular Pharmacology Fast Forward. Published on May 30, 2020 as DOI: 10.1124/mol.119.118786
This article has not been copyedited and formatted. The final version may differ from this version.

Compound comparisons using the net charge method led to the same conclusions as for the peak current method (Table 1). The number of oocytes (n) tested at each concentration was ≥4 and is given in Figure 2. Efficacy (I_{max}) estimates by peak current and net charge methods and potency (EC_{50}) estimates are presented in Tables 1 and 3 as arithmetic means ± one sample standard deviation. One way ANOVA of log_{10} transformed compound I_{max} and EC_{50} data was used to compare all analogs with nicotine, with Dunnett's multiple comparison post-test. Student's two-tailed t test was used to assess statistical significance between mean I_{max} and EC_{50} estimates for the two enantiomers of a compound.

Radioligand binding experiments

Rat brain membrane radioligand binding experiments were carried out essentially as previously described (Kem et al., 2004). Frozen adult male Sprague-Dawley rat brains (Pel-Freeze Biologicals, Rogers, AZ), after thawing on ice and being sliced into smaller pieces, were homogenized with a 30 ml Wheaton glass homogenizing tube and pestle in ice cold binding saline (120 mM NaCl, 5 mM KCl, 2 mM $CaCl_2$, 1 mM $MgCl_2$, 50 mM Tris-TrisHCl buffer, pH 7.4). After the homogenate was centrifuged at 14,600 x G for 10 min the resulting pellet was resuspended in fresh binding saline, homogenized, centrifuged again and the supernatant discarded. A protein assay (BCA, Pierce, Rockford, IL) was then performed to obtain the protein concentration of the washed and pellet-resuspended membranes, which were stored at -82°C before use. Each tube in the binding experiment received 100 µg of rat brain membrane protein.

Washed membranes from cultured TsA201 cells expressing human α4β2 nAChRs were also utilized to assess the nAChR affinities of nicotine and most nicotine analogs. Although these

Molecular Pharmacology Fast Forward. Published on May 30, 2020 as DOI: 10.1124/mol.119.118786
This article has not been copyedited and formatted. The final version may differ from this version.

cells are known to express both stoichiometries of this heteromeric receptor, nicotine binding curves in our study were well fitted assuming a single population displaying the characteristics of the highest affinity ($\alpha4_2\beta2_3$) form (Kuryatov et al., 2005). Cells at 80-90% confluence were collected with a disposable cell scraper after removing the culturing media from the flask (75 cm^2) and adding 6-10 ml of ice-cold Tris binding saline. The dislodged cells were collected in centrifuge tubes and spun down at 7,700 x G for 8 min. The loose pellet was collected and homogenized as described above for rat brain membranes; after a protein assay the washed membranes were stored at -85°C before use. For TsA201 cell membranes, 50 μg protein per tube were used for radioligand binding experiments. SH-EP1 cells expressing human α7 nAChRs were similarly cultured and their membranes (100 μg membrane protein per tube) were used in ^{125}I-α-BTX displacement assays (Zhao et al., 2003).

Radioligands selective for each nAChR subtype were obtained from Perkin Elmer Life and Analytical Sciences (Boston, MA). Using conditions reported to optimally measure α4β2 nAChR affinity, 1.0 nM ^{3}H-cytisine (34 Ci/mmol) displacement experiments were performed at 4^{o}C as previously reported by Pabreza et al. (1991). Measurements of α7 nAChR affinity were done by displacement of ^{125}I-α-BTX (136 Ci/mmol) binding; the final test ^{125}I-α-BTX concentration was 0.32 nM. These experiments required incubation for three hours at 37°C to assure equilibration. Membranes were suspended in binding saline containing 2 mg/ml bovine serum albumin (Sigma-Aldrich) to reduce non-specific binding. In each experiment, 48 disposable glass culture tubes each (total volume 0.50 ml) containing equal concentrations of cell membranes and radioligand but different concentrations of the compound of interest were always incubated together. For each radioligand, nonspecific binding was measured in the presence of a final concentration of 1 mM nicotine hydrogen tartrate (Sigma-Aldrich). After incubation, radioligand bound to

Molecular Pharmacology Fast Forward. Published on May 30, 2020 as DOI: 10.1124/mol.119.118786
This article has not been copyedited and formatted. The final version may differ from this version.

membranes in each tube was rapidly collected by vacuum filtration using a 48 position Brandel cell harvester (Gaithersburg, MD) and Whatman GF/C glass fiber filters that were pre-soaked in 0.5% polyethylenimine (Sigma-Aldrich) for 45 minutes to reduce nonspecific binding. The radiolabeled membranes were rapidly washed three times with 3 ml of ice-cold binding saline to remove the unbound radioligand. Filters containing ^{3}H-cytisine bound membranes were collected in 20 ml scintillation tubes and suspended in 8 ml 30% Scintisafe (Fisher Scientific, Atlanta, GA) scintillation fluid, then counted in a Beckman LS-6500 liquid scintillation counter after standing overnight. Filters containing ^{125}I-α-Btx bound membranes were placed in 4 ml gamma vials and counted in a Beckman Instruments (Fullerton, CA) 5500B gamma counter.

Displacement assay binding data were analyzed using Prism software. The mean counts per minute for each compound concentration were obtained from 4 replicates; the data was fitted to a sigmoidal concentration response curve for one site binding, from which the Hill slope (*n*) and IC_{50} were estimated as follows:

$$Y = Bottom + (Top-Bottom) / (1+10^{(X-Log\ IC50)n})$$

Top (of the curve) is the maximal specific binding plateau of radioligand, Bottom (of the curve) is the minimum specific binding plateau observed at high concentrations of the displacing ligand and X=Log (Compound), The K_d estimate for each radioligand and receptor, previously calculated from saturation binding experiments carried out using the same incubation conditions, was then used to calculate the equilibrium dissociation constant (K_i) value of the displacing ligand from the Cheng-Prusoff equation: $K_i = IC_{50}/[1+(Radioligand)/K_d]$. For [^{3}H]-cytisine, the binding K_d was 0.92 nM for rat brain membranes (RBM) and 0.48 nM for human α4β2 receptors expressed in TsA201 cell membranes. For ^{125}I-α-Btx, the K_d was 0.67 nM for RBM and 0.97

Molecular Pharmacology Fast Forward. Published on May 30, 2020 as DOI: 10.1124/mol.119.118786
This article has not been copyedited and formatted. The final version may differ from this version.

nM for human α7 receptors expressed in SH-EP1 cell membranes. One way ANOVA of $\log_{10}$ transformed compound mean K_is obtained from a number of individual experiments was used to compare analogs with nicotine, with Dunnett's multiple comparison post-test. A Student's two-tailed t test was used to assess statistical significance between the mean K_i estimates for cis and trans enantiomers of a compound.

Computer docking of nicotine analogs with nAChR model proteins

The protein crystal structures used for the *in silico* molecular docking were the *Lymnaea* Acetylcholine Binding Protein (AChBP) occupied by nicotine (Celie et al., 2004; Brookhaven Protein Data Bank accession code 1UW6) and a chimeric protein based on *Aplysia californica* AChBP containing binding site mutations to better resemble α7 nAChR, which was occupied by epibatidine. (Li et al., 2011, Brookhaven Protein Data Bank accession code 3SQ6). The molecular docking of all nicotine analogs was preceded by a two step optimization process aimed at obtaining consistent starting geometries. The random walk algorithm implemented in HyperChem v8.0 (HyperCube Inc., Gainesville, FL) was used to sample the potential energy surface to identify the lowest energy conformation of each molecule. One thousand conformations per molecule were generated by varying randomly all dihedral angles and using an acceptance energy cut-off of 6 kcal/mol above the best. All conformations with an energy difference of less than 0.05 kcal/mol were considered duplicates and hence only one was retained. Conformations with potentially "bad" (distance between any two atoms of less than 0.5Å) van der Waals contacts were discarded. The lowest energy conformation was further subjected to a QM optimization in GAMESS (Schmidt et al., 1993) using an STO-3G basis set to represent the wavefunction in the Hartree-Fock approximation. Molecular surface calculations

for each nicotine analog were made using MSROLL (Dock 6.5 Manual, UCSF, San Francisco, CA). Each molecular surface was used as input for the sphere generating program SPHGEN (Dock 6.5, UCSF). A cluster of 77 spheres that overlapped with the ligand (a nicotine or epibatidine molecule in the appropriate crystal structure) was manually selected to be the point of interest in the subsequent docking calculations. SHOWBOX was used to construct a 3-dimensional rectangle 6 Å in any direction from the sphere cluster. CHIMERA (Pettersen et al., 2004) was used to prepare each protein structure and convert the file type to the necessary Mol2 format. The box file was used as input for the GRID program which calculated the necessary information concerning the steric and electrostatic environment within the area of the box in the 1UW6 and 3SQ6 protein structures.

The nicotine analogs used as inputs for docking were energy minimized. DOCK6.5 (Allen et al., 2015) was then used to measure the predicted binding energies of the compounds within the binding pocket designated by the spheres. With ligand flexibility allowed, each compound was docked in a minimum of 20,000 orientations. Separate computations were done for docking to each of the following structures for the 1UW6 *Lymnaea* AChBP: (1) the water-free site, (2) the site containing persistent water LWA (Amiri et al., 2007) bound to the side chain oxygen on the complimentary surface, (3) the site containing LWB binding to Tyr 192 (Amiri et al., 2007) and finally, and (4) the site containing both of these waters. The fit of the lowest energy docked structure of each docked nicotine compound relative to the 1UW6 nicotine-AChBP structure was estimated by calculating the root mean square deviation for the 11 ring atoms of nicotine (See Table S2). The Internet-available program Coote was used for these determinations. To allow comparison of the compound free energies of binding (calculated from the observed binding affinities of the compounds for the two human receptors) with the docking energies predicted for

the two AChBPs, the predicted energies of the various analogs were first normalized with respect to the predicted nicotine docking energy. Then the predicted docking energies of the compounds were normalized with respect to the experimental free energy changes (calculated from their K_is) associated with their binding to SH-EP1 cell expressed human α7 receptors (Table 2). The experimental and predicted free energies (ΔGs) are presented in Table 5.

[Figure 2]

RESULTS

Concentration-response relationships for ACh, nicotine and the methylnicotines

We measured the functional properties of each methylnicotine, namely, the EC_{50} (inversely related to potency) and I_{max} (maximal ACh-normalized current), using *Xenopus* oocytes expressing human α7 or α4β2 nAChRs, to allow comparison of the compound with nicotine and its enantiomer. The concentration-current response curves of these two nAChRs for ACh and nicotine are shown in Figure S1. In addition, the same curve for nicotine, but without the standard error bars, is included as a dashed line in each concentration-response curve in Figure 2 to allow visual comparison with the nicotine analog curve. Because the α7 receptor is much less sensitive to ACh than the αβ42 receptor, the standard calibrating agonist was 1,000 μM ACh, but for the α4β2 nAChR it was 100 μM ACh. The two calibrating ACh concentrations were chosen to produce near-maximal responses that would not cause cumulative desensitization during the experiment.

Our concentration-response data for α7 receptors (Fig. 2, Table 1) includes both the more readily recorded peak current responses as well as currents integrated over the entire time of agonist response (net charge method). Both types of data were obtained from the same response.

Molecular Pharmacology Fast Forward. Published on May 30, 2020 as DOI: 10.1124/mol.119.118786
This article has not been copyedited and formatted. The final version may differ from this version.

When administered by standard methods of oocyte perfusion, including ours, the α7 peak current response for an administered concentration of agonist does not reflect the maximum degree of receptor activation possible with that agonist concentration, because receptor desensitization is more rapid than the solution change: the peak current occurs before the desired concentration is reached at the oocyte membrane (Papke and Thinschmidt, 1998). Nevertheless, the peak current response should allow us to quantitatively compare the α7 response of a methylated nicotine relative to that of its enantiomer or nicotine, since the diffusion limited rates of equilibration of these compounds with the receptor should be nearly the same. In support of this assumption, net charge responses obtained from the agonist pulses yielded the same conclusions as for the peak current responses, except that the net charge potency (EC_{50}) estimates were 2-3-fold smaller (See PC/NC ratios in Table 1).

[Tables 1&2]

Another consideration in the interpretation of the *Xenopus* oocyte functional data obtained with α4β2 nAChRs regards their subunit stoichiometry. Our functional measurements of the methylnicotine effects were nearly complete when the co-expression of α4β2 nAChRs with different stoichiometries and pharmacological properties was shown to be of general occurrence (Moroni et al., 2006). The $\alpha4_3\beta2_2$ low ACh-nicotine sensitivity receptor was reported to have a nicotine EC_{50} that is ~50X higher than for the high sensitivity $\alpha4_2\beta4_3$ receptor (Tavares et al., 2012). In our *Xenopus* oocyte experiments we routinely injected equal amounts of the two mRNAs. The nicotine concentration-response curve (Figure S1) that we obtained for α4β2 nAChRs was fitted well with Prism assuming a single population of α4β2 nAChRs**.** When the α4β2 mRNA ratio was either 4:1 or 1:4, we still obtained EC_{50} values for nicotine that were almost the same as when the mRNA ratio was 1:1 (Results not shown). The I_{max} value of nicotine

Molecular Pharmacology Fast Forward. Published on May 30, 2020 as DOI: 10.1124/mol.119.118786
This article has not been copyedited and formatted. The final version may differ from this version.

obtained with the 1:1 mRNA injected oocytes was nearly identical with that of the 100 μM ACh response, which was ~60% of the I_{max} for ACh. In published studies where α4 and β2 cDNAs were injected into the nucleus, the I_{max} for the high affinity form was 30-60% of the maximal ACh current response (Moroni et al., 2006). Thus, our I_{max} values for α4β2 receptors are consistent with previously published values for I_{max} obtained with the high affinity $\alpha4_2\beta2_3$ receptor. Our more recent experiments co-injecting an α4β2 concatamer mRNA with the β2 mRNA, which should yield only $\alpha4_2\beta2_3$ -like functional receptors (Fig S2), indicate that the near maximal concatameric responses for several key analogs were very similar to the maximum responses in our routine *Xenopus* experiments (Fig. S3), further supporting our contention that the latter primarily assessed the properties of the high affinity stoichiometry $\alpha4_2\beta2_3$ subtype.

The radioligand binding data measuring ligand affinity for α4β2 AChRs are unlikely to be affected by the presence of the low affinity $\alpha4_3\beta2_2$ receptors, since we measured displacement at such a low concentration (1 nM) of [^{3}H]-cytisine that few of these receptors would be occupied (Tavares et al., 2012; Moroni et al., 2006).

The variance estimates for the mean potencies (EC_{50}) and binding constants (K_is) of the compounds tended to increase as their mean values increased, so we used a $\log_{10}$ transformation of the estimates to better approximate a normal distribution of the individual estimates for a compound. This resulted in more similar variance estimates among the compounds and allowed one way ANOVA to be used to analyze comparisons of all compounds with nicotine.

Functional and radioligand binding data for each methylnicotine will now be presented and discussed in order of the five pyrrolidinium ring atoms 1' to 5' (Figure 1) numbered according to the International Union for Pure and Applied Chemistry nomenclature. Data for receptor α7

nAChRs will be presented initially since interactions of these compounds with this receptor subtype have not been previously reported.

[Tables 3 and 4]

1'-Methylnicotine and 1'-Ethylnornicotine

Ample evidence exists that the monocationic form of nicotine and of most other ionizable nAChR agonists is the form which binds to nAChRs with highest affinity (Barlow and Hamilton, 1962; Jeng and Cohen, 1980; Kem et al., 2004). Since the published pKa for ionization of the 1'N of nicotine (8.05, Fujita et al., 1971) is 0.65 units above physiological pH of 7.4 and the methylnicotine analogs were found to have similar pK_as (Table S1), our pharmacological data in Tables 1-6 largely reflect the properties of the monocationic species and are uncorrected for the small differences in ionization we observed for the 1'-ethyl-, 2'-methyl- and 5'-methylnicotine analogs (See Table S1 for estimation of the % monocationic species for compounds expected to show the largest differences in ionization).

We first examined the consequences of adding an additional methyl substituent to the 1'-N of nicotine and found major differences between the two receptors. For α7 receptors the agonist properties (Figure 2, Table 1) and binding affinities (Table 2) of the quaternary nitrogen analog, 1'-methylnicotinium iodide, were similar to those of nicotine, but they were diminished at α4β2 receptors (Figure 2, Tables 3 and 4). Thus, methyl quaternization of the pyrrolidinium nitrogen is well tolerated by α7 but not α4β2 nAChRs.

Replacing the 1'N-methyl group of nicotine with a larger alkyl group, as in 1'ethyl-nornicotine, also differentially affected agonistic properties at these two receptors. The ethyl substituent was relatively well tolerated by the α7 receptor: only the I_{max} was statistically

Molecular Pharmacology Fast Forward. Published on May 30, 2020 as DOI: 10.1124/mol.119.118786
This article has not been copyedited and formatted. The final version may differ from this version.

different from that of nicotine (Table 1). However, at α4β2 nAChRs 1'-ethyl-nornicotine potency and efficacy was inferior to that of nicotine (Table 3). We also found that racemic 1'propyl-nornicotine displayed almost a thousand-fold decrease in potency relative to nicotine at α4β2 receptors, in agreement with a previous study (Glassco et al., 1994) as well as a greatly reduced potency at α7 receptors (Results not shown). Thus, nicotine interaction with α4β2 receptors is particularly sensitive to the presence of bulky quantitatively alkyl groups at the 1'N position.

2'-Methylnicotines

Trans-2'-methylation produced unique changes relative to the other six carbon-methylated nicotines, who displayed reduced agonist properties relative to nicotine. 2'methylnicotine displayed agonist properties superior to nicotine at α7 receptors and was at least as active as nicotine at α4β2 receptors. α7 nAChR potency and equilibrium binding affinity (Table 1) were enhanced about 7fold for the human receptor in comparison with nicotine. At the α4β2 receptor, 2'-methylnicotine potency and I_{max} were not statistically different from nicotine (Table 3). The small increase in binding affinity at the α4β2 receptor was only statistically significant for the human receptor (Table 4). Our data for 2'-methylnicotine binding to rat brain α4β2 receptors was consistent with the data of Wang et al. (1998) for racemic 2'-methylnicotine, taking into consideration that our 2'-methyl(S)nicotine has a much higher (>40 fold) higher binding affinity than 2'-methyl(R)nicotine (Kem, unpublished results).

3'-Methylnicotines

Cis-3'-methylnicotine displayed less potency (~3 fold at α7 and ~10 fold at α4β2 receptors) relative to nicotine (Figure 2, Tables 1 and 3). There was also a statistically significant

(~2 fold) decrease in the α4β2 receptor I_{max}. Cis-3'-methylnicotine displayed less affinity for α7 (approximately 4 fold for rat and 8 fold for human) and α4β2 (approximately 200 fold less for rat and 400-fold less for human) receptors relative to nicotine (Tables 2 and 4). While the affinity of trans-3'methylnicotine for the α7 receptor was similar to that of nicotine, its affinity for α4β2 receptors was ≥30 fold less than for nicotine.

4'-Methylnicotines

At both receptors (especially the α7) the efficacies of both 4'-methylnicotines were greatly reduced relative to nicotine (Figure 2, Tables 1 and 3). Whereas the potencies of the two enantiomers were inferior to that of nicotine at α7 receptors, on the human α4β2 receptor the potencies were not significantly different from that of nicotine. Relative binding affinities of the two enantiomers at the two receptors differed: at both α7 receptors the cis enantiomer displayed the highest affinity, but at rat and human α4β2 receptors the trans-enantiomer displayed the highest affinity.

5'-Methylnicotines

Analysis of the pharmacological properties of cis-5'-methylnicotine revealed its limited ability to interact with α4β2 receptors. Agonist potency was reduced >700 fold and I_{max} >100 fold (Table 3). The binding K_i's for rat and human α4β2 receptors also were increased >2,000 fold and >700 fold, respectively (Table 4). Previous radioligand binding studies also indicated that methylation at this position had detrimental effects on nicotine binding affinity for rat brain high affinity (α4β2) receptors and that the binding K_i of trans-5'-methyl-nicotine was less affected than that of the cis-form (Lin et al., 1994; Wang et al., 1998).

Molecular Pharmacology Fast Forward. Published on May 30, 2020 as DOI: 10.1124/mol.119.118786
This article has not been copyedited and formatted. The final version may differ from this version.

While cis-5'-methylnicotine also displayed the greatest reduction in interaction with α7 receptors, trans-5'-methylnicotine was a relatively potent agonist, potency decreasing only 2-3 fold and I_{max} decreasing ~1.5 fold relative to nicotine (Table 1). Binding affinities for the human and rat α7 nAChRs were only decreased ~3 fold relative to nicotine (Table 2).

[Figure 3]

Relationships between receptor affinity and receptor potency

Compound $EC_{50} = K_d / (E+1)$, where Kd is the equilibrium dissociation constant for initial binding to the inactive state and E is the equilibrium constant associated with receptor activation (Auerbach et al., 2016). If K_i estimates are related to the K_d, then our EC_{50} estimates might show some relationship to the K_is, at least for compounds displaying low E values. We plotted K_i versus EC_{50} estimates for each alkylnicotine to determine whether they might be related (Figures 3A and C). We used EC_{50} estimates obtained with the net charge method of analysis for EC_{50} and I_{max} characterization of the functional properties of the human α7 receptor in this Figure. Both the α7 and α4β2 plots showed a relatively strong correlation between these two variables (Part A, α7 correlation coefficient $r^2 = 0.90$; Part C, α4β2 $r^2 = 0.61$). Since the α7 net charge determined EC_{50}s (Table 1) were ~3 fold less than the peak current EC_{50} estimates, using our standard 2 sec agonist exposure (and ~10 fold less for a 20 second exposure, Kem, unpublished results), the actual α7 receptor EC_{50} for each compound may be as much as 10 fold less than the peak current EC_{50} reported in Table 1 and used in Part A of this Figure.

It was recently reported that there is a linear relationship between Log I_{max} and Log EC_{50} for agonists at the mouse neuromuscular nAChR--that high efficacy is directly correlated with high potency (Auerbach, 2016). In spite of the differences in how efficacy was measured (single

Molecular Pharmacology Fast Forward. Published on May 30, 2020 as DOI: 10.1124/mol.119.118786
This article has not been copyedited and formatted. The final version may differ from this version.

channel recording in the Auerbach et al. study and oocyte net charge response here, a similar correlation was observed with our α7 data (Figure 3B, r^2=0.67). In Figure 3B the I_{max} estimates for the most efficaceous compounds (2'MeNic, 1'MeNic and Nic) are very similar, though their EC_{50}s differ considerably, which would not be predicted from the Auerbach equation; it seems likely that desensitization may limit the I_{max}s measured for these highly potent agonists under our experimental conditions. In contrast to the α7 plot in 3B, the α4β2 plot showed much more scatter when plotted in an identical fashion (Figure 3D, r^2=0.24).

Modeling methylnicotine interaction with the molluscan ACh binding proteins

Since high resolution crystal structures of the two nAChRs are still unavailable, we attempted to predict the binding poses and relative docking free energies of the various methylnicotines using the Brookhaven Protein Data Bank *Lymnaea* AChBP-nicotine 1UW6 structure (Celie et al., 2004) and the mutated *Aplysia californica* AChBP-epibatidine 3SQ6 structure where the binding site was mutated to be similar to the α7 site (Li et al., 2011). In the 1UW6 structure the cis- side of the nicotine pyrrolidinium ring comes in closest proximity with the AChBP Trp143 indole side chain and the 1'N proton is also very near (2.6 Å) the Trp143 peptide carbonyl group, and is assumed to form an H-bond with it (Celie et al., 2004). In contrast, the 2'-carbon of nicotine is not in close contact with any non-water atoms in the AChBP binding site. Actually, the 2'-methyl is oriented towards the disulfide bond between the vicinyl half-cystines in the C-loop. The structures of the various methylnicotines (as monocations) were energy-minimized and docked to both AChBPs after removing the crystallized ligands from their respective ACh binding sites. The relative energies for docking the various methyl-nicotines (Table 5) to both AChBP structures predicted many of the differences in binding affinity that were observed, particularly when two of the most persistently

Molecular Pharmacology Fast Forward. Published on May 30, 2020 as DOI: 10.1124/mol.119.118786
This article has not been copyedited and formatted. The final version may differ from this version.

bound water molecules in the *Lymnaea* AChBP-nicotine complex (Amiri et al., 2007) were retained within the binding site during docking (See Table S2 for fit estimates). For the 3'- and 5'-methylnicotines the docking score of the cis-methyl enantiomer predicted a less favorable free energy of binding relative to the trans enantiomer, and cis-5'-methylnicotine was predicted to have the least favorable free energy of binding of all the methyl analogs to both AChBPs (Table 5). The nicotine compound predictions for the *Aplysia* AChBP-α7 chimera binding site, containing no water molecules, were similar to those obtained for the *Lymnaea* AChBP.

Comparison of free energy changes associated with compound binding to human nAChRs with predicted free energy changes for binding to AChBPs

The ΔGs (Table 5) of the various analogs relative to the ΔG for nicotine binding at the same receptor site, expressed within the parentheses as a percent change, are most salient. The relative ΔG changes associated with methylation were much greater for α4β2 receptors than for α7 receptors. The major exception was 2'-methylnicotine, which actually showed a greater free energy decrease (lower K_i) relative to nicotine at the α7 receptor. This was only predicted for the *Aplysia* AChBP-α7 chimera, whose orthosteric binding site most resembles the α7 binding site. Another important observation was that the free energy of binding difference (-1.9 Kcal/mol) for nicotine, between the human α4β2 receptor (ΔG = -10.8 Kcal/mol) and the α7 receptor (ΔG = -8.9 Kcal/mol), almost disappeared in free energy comparisons for most other analogs other than the 1'N-methynicotinium and 1'N-ethylnornicotine. This important observation will be discussed later.

[Table 5]

Molecular Pharmacology Fast Forward. Published on May 30, 2020 as DOI: 10.1124/mol.119.118786
This article has not been copyedited and formatted. The final version may differ from this version.

Influence of methyl substituent configuration on receptor interaction in other methylated nicotine analogs

Abreo et al. (1996) synthesized and tested the nicotine analog A84543 in which an oxymethylene group forms a bridge between the 3-pyridyl ring and the 2'(S) position of the pyrrolidinium ring so that the pyridyl ring retains the same chirality as in nicotine. This compound displayed very high affinity and potency at α4β2 receptors, exceeding that of nicotine, indicating that this receptor not only tolerates a greater distance between the two nicotine ring N atoms but binds this compound more readily than nicotine. To determine whether A84543 would be similarly affected by 5'-methylation, we synthesized (See Supplement) and tested the two 5'-methylA84543 diastereomers. The rat brain α4β2 receptor affinity (Table 6) of trans-5'-methylA84543 was 7-fold higher than the cis-5'methyl-A84543. The rat brain high affinity receptor K_i for A84543 has been reported to be 0.15±0.01 (Abreo et al., 1996) and 3.44±0.40 nM (Ogunjirin et al., 2015) and the α7 receptor K_i was reported to be 340 ±50 nM (Ogunjirin et al., 2015). While the difference we observed between the two methylated A84543 enantiomers was approximately 10X less than it was for the 5'methyl-nicotines, it is clear that the preferential binding of the trans-5'-methylnicotine also applies to trans-5'methyl A85443. Like A84543, both methyl enantiomers interacted with α7 receptors with much lower affinity relative to α4β2 receptors, with the cis- enantiomer showing the least affinity and potency (Table 6). The efficacies of trans-5'methyl-A84543 (Figure 4) at human α7 and α4β2 receptors were similar to those of trans-5'methylnicotine (Tables 1 and 3).

Since we had prepared racemic 3'-and 5'methylnicotines and then separated the diastereomeric (R)- and (S)-methylnicotines, this afforded the opportunity of determining whether the relative or absolute configurations of these two methyl substituents are critical for

Molecular Pharmacology Fast Forward. Published on May 30, 2020 as DOI: 10.1124/mol.119.118786
This article has not been copyedited and formatted. The final version may differ from this version.

optimal interaction with the receptors. Our binding data shows that at the 3'-position the same relative configuration (trans) allows the highest affinity, irrespective of the pyridyl ring substituent configuration. However, it is the absolute configuration of the 5'-methyl substituent that determines relative activity, since the substituent in cis-5'methyl-(R)nicotine has the same absolute configuration as the methyl in tran-5'methyl-(S)nicotine.

[Figure 4, Table 6]

DISCUSSION

Dominant role of the cationic N-alkyl moiety

Ionization of the most basic N atom is essential for efficient binding of nicotine and most nicotinoids to various AChRs and AChBPs. The pyrrolidinyl N in nicotine has been reported to possess a pK_a of 8.05 and a pyridyl ring N pK_a of 3.85 (Fujita et al., 1971). Thus, at physiological pH there will be a mixture of the monocationic and unionized pyrrolidinyl forms and their relative solution concentrations will depend upon the pH. Under the ionic strength conditions of our radioligand binding measurements, the nicotine pK_a1 was 8.00 and its ionization was 80% at pH 7.4 (Table S1). The pK_a1 of the pyrrolidinium N was enhanced the most (to 8.44) by replacing the 1'N-methyl with an ethyl group. Methylating the 2' or 5'positions produced very small increases in ionization at pH 7.4. Methylation at the 3' or 4' position would not be predicted to have a significant inductive effect on the pK_a1.

Adding an additional methyl to the 1'N of nicotine greatly diminished interaction with the α4β2 receptor without much effect on interaction with the α7 receptor. Substituting the larger ethyl moiety for the 1'N-methyl group, as in 1'N-ethylnornicotine, was deleterious for interaction with both receptors, especially the α4β2 receptor. Formation of the 1'N-Trp B

Molecular Pharmacology Fast Forward. Published on May 30, 2020 as DOI: 10.1124/mol.119.118786
This article has not been copyedited and formatted. The final version may differ from this version.

carbonyl hydrogen bond seems to be important for nicotine binding to α4β2 receptors (Xiu et al., 2009; Puskar et al., 2011). The high affinity of nicotine for the α4β2 receptor may at least partially be due to this hydrogen bond, which seems less important for its interaction with the α7 nAChR subtype and may not be essential (Puskar et al., 2011; van Arnam et al., 2013**).** The lesser effects on α7 interaction of these two 1'-N modifications suggests that a small increase in bulk of the pyrrolidinium group does not adversely affect cation-π binding. The highly detrimental influence of increasing the bulk of substituents at the 1'N for α4β2 receptor interaction may be due to these bulky substituents interfering with formation of this hydrogen bond.

2'Methylation uniquely increases interaction with the α7 receptor without adversely affecting interaction with the α4β2 nAChR

Unexpectedly, methylation at the 2'-carbon, which also connects the two rings, significantly enhances binding and agonist potency at the α7 nAChR without significantly affecting interaction with the α4β2 nAChR. The 2'methyl may form a hydrophobic interaction with some group and that may favor formation of an H bond between the 1'NH+ and the receptor, which otherwise seems to be absent. If binding site waters are present in the vicinity of the 1'NH of nicotine, they might be displaced by a methyl substituent like the 2'methyl (Barratt et al., 2006; Leung et al., 2012). Water molecules are present in the agonist-bound AChBP as well as in the agonist-free state of the AChBP binding site (Celie et al., 2004; Amiri et al., 2007) and it has been found (Forli and Olson, 2011; this study) that better docking predictions can be obtained when persistent water molecules observed in the nicotine-AChBP crystal binding site are included in the computer docking. The actual basis for the potentiating effect of the 2'methyl substituent can only be determined by additional experimental and computational studies.

Molecular Pharmacology Fast Forward. Published on May 30, 2020 as DOI: 10.1124/mol.119.118786
This article has not been copyedited and formatted. The final version may differ from this version.

3'Cis-methylation reduces agonist activity more than 3'trans-methylation

Since the pyrrolidinium 3'carbon is next to the inter-ring bonding 2'carbon, it was predicted that its methylation would alter the energy profile for inter-ring torsion and might even prevent the compound from attaining an optimal conformation for agonistic binding and to the receptor. While both 3'-methylnicotines were less active than nicotine, we found that that trans-3'-methylnicotine was significantly more active than cis-3'-methylnicotine at both receptors. The thermodynamically preferred inter-ring angles for cis-3'- and trans-3'-methylnicotine and for nicotine are predicted to be very similar, but the energy barrier for rotation around the C2'-C3 bond is much higher (60 Kcal/mol) for cis-3'-methylnicotine compared with 14 Kcal/mol for trans-3'-methylnicotine (Seeman, 1984). One possibility is that the two rings must be able to move with respect to each other in the binding or receptor activation processes, and the presence of the 3'methyl substituent to varying degrees inhibits these movements. The data in Table 6, indicating that the relative configuration of the 3'-methyl group is more important for activity and binding than its absolute configuration, is consistent with this interpretation.

5'Cis-methylation causes a drastic loss of activity at both nAChRs

The 5' position of the pyrrolidinium ring is adjacent to the 1'N hydrogen, which H-bonds to the peptide carbonyl of Trp 143 at the *Lymnaea* AChBP and by inference at Trp B of the α4β2 nAChR (Xiu et al., 2009; Blum et al., 2010). The H-bond does not seem to be present or very strong at α7 receptors, at least for ACh, epibatidine and varenicline (van Arnum et al., 2013). Since the 5'cis-hydrogen of nicotine abuts the Trp 143 side chain in AChBP, we suggest that cis-methylation at this site significantly lowers the free energy change associated with nicotine's H-bonding to the equivalent Trp B (residue 149) in the α4β2 receptor. Theoretical calculations of the positive charge density of the various carbon atoms in the pyrrolidinium ring of nicotine

Molecular Pharmacology Fast Forward. Published on May 30, 2020 as DOI: 10.1124/mol.119.118786
This article has not been copyedited and formatted. The final version may differ from this version.

indicate that the positive charge is less centered on the pyrrolidinyl N than on the three C atoms (1', 2' and 5') attached to the nicotine 1'N (Elmore and Dougherty, 2002). Regardless of mechanism, the significant dimunition in 5'cis-methyl nicotine binding to both receptors indicates that the 5'- carbon occupies a very critical position that can exert much control of nicotine's interaction with these receptors. The superior activity of 5'trans-methylA84543 relative to 5'cis-methylA84543 (Table 6 and Figure 4) is consistent with the notion that the binding orientation this compound, though it contains an oxymethylene bridge between the pyridyl and pyrrolidinyl rings, is very similar to that of nicotine. Our data regarding the relative affinities of the 5'methyl(R)nicotine enantiomers indicates that it is the absolute configuration of the 5'methyl group that determines the relative affinities of these enantiomers for both receptors.

The effects of 5'methylation were greatest on nicotine's interaction with the α4β2 nAChR receptor. Based on the earlier radioligand binding studies with some of these nicotine analogs on α4β2 receptors, we anticipated that all methylations would diminish nicotine's agonistic properties. Our radioligand binding data demonstrated a preferential reduction in binding of the 3'cis- and 5'cis-methylated nicotines on both receptors, as well as for cis-4'-methylnicotine binding to the rat α4β2 (but not the α7 receptor). While the molecular basis for this behavior is not yet known, it suggests that interaction of the cis side of the pyrrolidinium ring with a part of the receptor is of paramount importance. It seems likely, based on the close proximity of the cis-side of the pyrrolidinium ring to Trp 143 in AChBPs and Trp B in the α4β2 x-ray structure (Perez et al., 2016), that cis methylation generally interfers with nicotine's interaction with this component of the aromatic "box". The lesser influence of cis-methylation on interaction with the α7 receptor could be due to the lesser importance of 1'NH+ hydrogen-bonding to Trp B and/or

the cation-π bonding forces between nicotine and this receptor being directed towards an adjacent Tyr in the aromatic box (Dougherty et al., 2011).

The docking of nicotine and its methylated analogs to AChBPs

The solution conformation of nicotine has been the subject of extensive experimental and theoretical investigations over the last few decades. NMR and theoretical studies have provided strong evidence that the preferred conformation of nicotine in aqueous solution is one in which the two rings of nicotine are twisted with respect to each other (Chynoweth et al., 1973; Pitner et al., 1978; Elmore and Dougherty, 2002). The four carbon atoms of the pyrrolidinium ring are in a relatively planar "envelope" conformation in crystalline and aqueous solution conditions. While the 1'N-methyl group of nicotine is capable of inversion, its trans orientation with respect to the pyridyl ring substituent is of slightly lower free energy in solution. The relative positions of the two rings of nicotine in the *Lymnaea* AChBP crystal structure are very similar to that observed for nicotine in solution or in a vacuum, except that the N-methyl is cis- with respect to the pyridyl ring (Celie et al., 2004).

Comparison of the calculated, experimental free energies of binding of the various analogs (Table 5) revealed some interesting similarities in the binding energies of the 1'- 3'-, 4', and 5'-methylated nicotines on both receptors. Although the functional properties differed, the measured -ΔG (Kcal/mol) values for 1'methylnicotinium, both 3'-methylnicotines and both 5'-methylnicotines were very similar for the two receptors. It is tempting interpret the much reduced binding of these analogs to the α4β2 receptor, such that they bind with similar affinity to

Molecular Pharmacology Fast Forward. Published on May 30, 2020 as DOI: 10.1124/mol.119.118786
This article has not been copyedited and formatted. The final version may differ from this version.

the α7 receptor, as being due to their inability to form the 1'NH hydrogen bond with the Trp B peptide carbonyl in this receptor.

Concluding Remarks

While similarities in methylation effects are also of general interest for understanding the interaction of nicotine with AChRs, if selective enhancement or dimunition of activity at one of the nAChR subtypes is desired in the design of new nicotinic drugs, then the differences become of paramount interest. CNS drug design has largely focused on development of drug candidates selective for either α4β2 or α7 receptors. Drug design using nicotine as the lead compound has focused on improving selectivity for the high affinity heteromeric receptor subtypes, but our study demonstrates that the nicotine scaffold is capable of being modified so as to increase its interactions with α7 nAChRs. Enhancing cognitive function by separately stimulating a particular brain nAChR, α4β2 or α7, has been a therapeutic goal for at least two decades, but a maintained occupation of either α4β2 or α7 receptors seems to produce suboptimal stimulation of cognitive processes in humans (Kem et al., 2017). The two major nAChR subtypes are widely expressed in the brain, often in different parts of the same neuron or within different neurons in a common circuit. Our data for 2'-methylnicotine suggests that it may be possible to concurrently stimulate both receptors at an appropriate brain concentration. A dual receptor stimulation strategy might provide a more powerful cognitive effect than when only one of the receptor subtypes is stimulated. There are some recent studies that suggest that this may be promising

approach, as long as adverse effects exerted through autonomic or neuromuscular nAChRs can be avoided (Sun et al., 2019; Potasiewicz et al., 2019).

By measuring binding affinities of the various nicotine analogs on both rat and human forms of each receptor, we have shown that these compounds display almost identical interactions with receptors of the two species. Some agonists, such as DMXBA (GTS-21), display differences in their interactions with rat and human α7 nAChRs (Kem et al, 2004). The nearly identical binding behavior of the nicotine analogs in receptors of both species should facilitate behavioral predictions for humans based on rat models.

Some of the nicotine analogs considered in this paper have already been tested in rats and found to reduce nicotine self-administration (Rowland et al., 2008). Of particular interest is the ability of trans-5'-methylnicotine to inhibit self-administration of nicotine, in spite of its greatly diminished affinity for α4β2 receptors. We recently learned that this compound is a relatively potent partial agonist at α6β2* nAChRs (Kem et al., unpublished results). Thus, some of the methylnicotines may interact differently with other nAChR subtypes than would be predicted from our current studies with the two major brain nAChRs.

Our study has revealed important differences as well as similarities in the orthosteric binding sites of α4β2 and α7 nAChRs that may be useful in designing new drug candidates based on the nicotine scaffold. "Dougherty" type analyses (Cashin et al., 2005; Davis and Dougherty, 2015) investigating the effects of introducing electron-withdrawing substituents on Trp B and other members of the binding site "aromatic box" are likely to provide additional insights into the interactions of some of these methylnicotines and how they differ from nicotine. Crystal structures, especially of 2'methyl- and 5'trans-methylnicotines bound to AChBPs, α4β2 and α7 receptors, would also be informative.

Molecular Pharmacology Fast Forward. Published on May 30, 2020 as DOI: 10.1124/mol.119.118786
This article has not been copyedited and formatted. The final version may differ from this version.

Molecular Pharmacology Fast Forward. Published on May 30, 2020 as DOI: 10.1124/mol.119.118786
This article has not been copyedited and formatted. The final version may differ from this version.

REFERENCES

Abreo MA, Lin N-H, Garvey DS, Gunn DE, Hettiner A-H, Sasicak JT, Pavlik PA, Martin YC, Donnelly-Roberts DL, Anderson DJ, Sullivan JP, Williams M, Arneric SP, and Holladay MW (1996) Novel 3-pyridyl ethers with subnanomolar affinity for central neuronal nicotinic acetylcholine receptors. J Med Chem 39:817-825.

Allen WJ, Balius TE, Mukherjee S, Brozell SR, Moustakas DT, Lang PT, Case DA, Kuntz ED, and Rizzo RC (2015) DOCK 6: Impact of new features and current docking performance. J. Comput Chem 36:1132-1156.

Amiri S, Sansom MSP, and Biggin PC (2007) Molecular dynamics studies of AChBP with nicotine and carbamylcholine: the role of water in the binding pocket. Prot Engr Design Selection 20:353-359**.**

Auerbach A (2016) Dose-response analysis when there is a correlation between affinity and efficacy. Mol Pharmacol 89:297-302.

Barratt E, Bronowska A, Vondrasek, Cerny J, Bingham R, Phillips S, and Homans SW (2006) Thermodynamic penalty arising from burial of a ligand polar group within a hydrophobic pocket of a protein receptor. J Mol Biol 362:994-1003.

Barlow RB, and Hamilton JT (1962) Effects of pH on the activity of nicotine and nicotine monomethiodide on the rat diaphragm preparation. Brit J Pharmacol 18:543-549.

Bertrand D, Lee C-H, Flood D, Marger F, and Donnelly-Roberts A (2015) Therapeutic potential of α7 nicotinic acetylcholine receptors. Pharmacol Rev 67:1025-1073.

Black JW, Dunan AM, Durant CJ, Ganelli CR, and Parsons WM (1972) Definition and antagonism of histamine H2-receptors. Nature 236:385-390.

Blum AP, Lester HA, and Dougherty DA (2010) Nicotinic pharmacophore: The pyridine N of nicotine and carbonyl of acetylcholine hydrogen bond across a subunit interface to a backbone NH. Proc Nat Acad Sci USA 107:13206-13211.

Bouzat C, Lasala M, Nielsen BE, Corradi J, and Esandi MDC (2018) Molecular function of α7 receptors as drug targets. J Physiol 596:1847-1861.

Braumann T, Nicolaus G, Hahn W, and Elmenhorst H (1990) N'-ethylnornicotine from burley tobacco. Phytochem 29:3693-3694.

Burghaus L, Schutz U, Krempel U, Lindstrom J, and Schroder H (2003) Loss of nicotinic acetylcholine receptor subunits alpha4 and alpha7 in the cerebral cortex of Parkinson patients. Parkinson and Related Disorders 9:243-246.

Cashin AL, Petersson EJ, Lester HA, and Dougherty DA (2005) Using physical chemistry to differentiate nicotinic cholinergic agonists at the nicotinic acetylcholine receptor. J Amer Chem Soc 127:350-356.

Celie PHN, van Rossum-Fikkert SE, van Kijk WJ, Brejc K, Smit AB, and Sixma, T.K. (2004) Nicotine and carbamylcholine binding to nicotinic acetylcholine receptors as studied in AChBP crystal structures. Neuron 41:907-914.

Changeux JP (2012) The nicotinic acetylcholine receptor: The founding father of the pentameric ligand-gated ion channel superfamily. Biochem 287:40207-40215.

Clayton PM, Vas CA, Bui TT, Drake AF, and McAdam K (2013) Spectroscopic studies on nicotine and nornicotine in the UV region. Chirality 25:288-293.

Chynoweth KR, Ternai B, Simeral LS, and Maciel GE (1973) Nuclear magnetic resonance studies of the conformation and electron distributions in nicotine and in acetylcholine. Mol Pharmacol 9:144-151.

Dellisanti CD, Yao Y, Stroud JC, Wang Z, and Chen L (2007) Crystal structure of the extracellular domain of nAChR α1 bound to α-bungarotoxin at 1.94 Å resolution. Nat Neurosci 10:953-962.

Davis MR, and Dougherty DA (2015) Cation-π interactions: computational analyses of the aromatic box motif and the fluorination strategy for experimental evaluation. J Phys Chem 17:29262-29270.

Dukat M, Fiedler W, Dumas D, Damaj I, Martin BR, Rosecrans JA, James JR, and Glennon RA (1996) Pyrrolidine-modified and 6-substituted analogs of nicotine: a structure-affinity investigation. Eur J Med Chem 31:875-888.

Elmore DE, and Dougherty DA. (2000) A computational study of nicotine conformations in the gas phase and in water. J Org Chem 65:742-747.

Forli S, and Olson AJ (2011) A force field with discrete displaceable waters and desolvation entropy for hydrated ligand docking. J Med Chem 55:623-638.

Fujita T, Nakajima M, Soeda Y, and Yamaoto I (1971) Physicochemical properties of biological interest of nicotine and its related compounds. Pest Biochem Physiol *1*:151-162.

Glassco W, May EL, Damaj M I, and Martin BR (1994). *In vivo* and *in vitro* activity of some N-substituted (±)-nornicotine analogs. Med Chem Res 4:273-282.

Jeng AY, and Cohen JB (1980) Agonists of *Torpedo* nicotinic receptors: Essential role of a positive charge. Ann NY Acad Sci 358:370-373.

Kem WR, Mahnir VM, Prokai L, Papke RL, Cao X, LeFrancois S, Wildeboer K, Prokai-Tatrai K, Porter-Papke J, and Soti F (2004) Hydroxy metabolites of the Alzheimer's drug candidate 3-[2,4-dimethoxy)benzylidene]-anabaseine dihydrochloride (GTS-21): their molecular properties, interactions with brain nicotinic receptors and brain penetration. Mol Pharmacol *65*:56-67.

Kem WR, Olincy A, Johnson L, Harris J, Wagner BD, Buchanan RW, Christians U, and Freedman R (2017) Pharmacokinetic limitations on effects of an alpha7-nicotinic receptor agonist in schizophrenia: Randomized trial with an extended-release formulation. Neuropsychopharmacol 2017:1-7.

Kim KH, Lin N-H, and Anderson DJ (1996). Quantitative structure-activity relationships of nicotine analogues as neuronal nicotinic acetylcholine receptor ligands. Bioorg Med Chem *4*:2211-2217.

Kuryatov A, Luo J, Cooper J, and Lindstrom J (2005). Nicotine acts as a pharmacological chaperone to upregulate human alpha4 beta2 acetylcholine receptors. Mol Pharmacol 68:1839-1851.

Leong CS, Leung SF, Tirado-Rives J, and Jorgensen WL (2012) Methyl effects on protein-ligand binding. J Med Chem 55: 4489-4500.

Li S-X, Huang S, Bren N, Noridomi K, Dellisanti CD, Sine SM, and Chen L (2011) Ligand-binding domain of an α7-nicotinic receptor chimera and its complex with agonist. Nature Neurosci 14:1253-1260.

Lin N-H, Carrera Jr GM, and Anderson DJ (1994) Synthesis and evaluation of nicotine analogs as neuronal nicotinic acetylcholine receptor ligands. J Med Chem *37*:3542-3553.

Martin LF, Kem WR, and Freedman R (2004) Alpha-7 nicotinic receptor agonists: Potential new candidates for the treatment of schizophrenia. Psychopharmacol 174:54-64.

Morales-Perez CL, Noviello CM, and Hibbs RE (2016) X-ray structure of the human α4β2 receptor. Nature 538:411-418.

Moretti M, Zoli M, George AA, Lukas RJ, Pistillo RJ, Maskos F, Whiteaker P, and Gotti C (2014) The novel alpha7beta2 nicotinic acetylcholine receptor subtype is expressed in mouse and human basal forebrain: biochemical and pharmacological characterization. Mol Pharmacol 86:306-317.

Moroni M, Zwart R, She E., Cassels BK, and Bermudez I (2006) α4β2 receptors with high and low ACh sensitivity: Pharmacology, stoichiometry, and sensitivity to long-term exposure to nicotine. Mol Pharmacol 70:755-768.

Moustakas DT, Lan PT, Pegg S, Pettersen E, Kuntz ID, Brooijmans N, and Rizzo RC (2006) Development and validation of a modular, extensible docking program: DOCK 5. J. Comput Aided Mol Des 20:601-619.

Nelson ME, Kuryatov A, Choi CH, Zhou Y, and Lindstrom J (2003) Alternate stoichiometries of α4β2 nicotinic acetylcholine receptors. Mol Pharmacol 63:332-341.

Nielsen BE, Minguez T, Bermudez I, and Bouzat C (2018) Molecular function of the novel α7β2 nicotinic receptor. Cell Mol Life Sci 75:2457-2471.

Ogunjirin AE, Fortunak JM, Brown L, Xiao Y, and Davila-Garcia MI (2015) Competition, selectivity and efficacy of analogs of A-84543 for nicotinic acetylcholine receptors with repositioning of pyridine nitrogen. Neurochem Res 40:2131-2142.

Pabreza L, Dhawan S, and Kellar KJ (1991) [^{3}H]cytisine binding to nicotinic cholinergic receptors in brain. Mol Pharmacol 39:9-12.

Papke RL, and Thinschmidt J (1998) The correction of alpha7nicotinic acetylcholine receptor concentration-response relationships in *Xenopus* oocytes. Neurosci Lett 256:163-166.

Peng J-H, Lucero L, Fryer J, Herl J, Leonard SS, and Lukas RJ (1999) Inducible, heterologous expression of human α7-nicotinic acetylcholine receptors in a native nicotinic receptor-null human clonal line. Brain Res 825:172-179.

Pettersen EF, Goddard TD, Huang CC, Couch GS, Greenblatt DM, Meng EC, and Ferrin T. (2004) UCSF Chimera-a visualization system for exploratory research and analysis. J Comput Chem 25:1605-1612.

Pitner TP, Edwards WBIII, Bassfield RL, and Whidby JF (1978) The solution conformation of nicotine. A ^{1}H and ^{2}H nuclear magnetic resonance investigation. J Amer Chem Soc 100:246-251.

Potasiewicz A, Golebiowska J, Popik P, and Nikiforuk A (2019) Procognitive effects of varenicline in the animal model of schizophrenia depend on α4β2 and α7 nAChRs nicotinic acetylcholine receptors. J Psychopharmacol 33:62-63.

Puskar NL, Xiu X, Lester HA, and Dougherty DA (2011) Two neuronal nicotinic acetylcholine receptors, α4β4 and α7, show differential agonist binding modes. J Biol Chem 286:14618-14627.

Rouchaud A, and Kem WR (2012) Synthesis of racemic 2'substituted nicotines. J Heterocyclic Chem 49:161-166.

Rowland NE, Robertson K, Soti F, and Kem WR (2008) Nicotine analog inhibition of nicotine self-administration. Psychopharmacol 199:605-613.

Schmidt MW, Baldridge K., Boatz JA, Elbert ST, Gordon MS, Jensen JH, Koseki S, Matsunaga N, Nguyen KA, Su S, Windus TL, Dupuis M, and Montgomery JA (1993) General Atomic and Molecular Electronic Structure System. J Comput Chem 14:1347-1363.

Seeman JI (1984) Recent studies in nicotine chemistry. Conformational analysis, chemical reactivity studies and theoretical modeling. Heterocycles 22:165-193.

Sun JL, Stokoe SJ, Roberts JP, Sathler MF, Nip KA, Shou J, Ko K, Tsunoda S, and Kim S. (2019) Co-activation of selective nicotinic acetylcholine receptors is required to reverse beta amyloid-induced Ca^{2+} hyperexcitation. Neurobiol Aging 164:166-177.

Tang Y, Zielinski WL, and Bigott HM (1998) Separation of nicotine and nornicotine enantiomers via normal phase HPLC on derivatized cellulose chiral stationary phases. Chirality 10:364-369.

Tavares XS., Blum AP, Nakamura DT, Puskar NL, Shanata JA, Lester A., and Dougherty DA (2012) Variations in binding among several agonists at two stoichiometries of the neuronal, α4β2 nicotinic receptor. J Am Chem Soc 134:11474-80.

Testa B, and Jenner P (1973) Circular dichroic determination of the preferred conformation of nicotine and related chiral alkaloids in aqueous solution. Mol Pharm 9:10-16.

Van Arnam EB, Blythe WE, Lester HA, and Dougherty D (2013) An unusual pattern of ligand-receptor interactions for the α7 nicotinic acetylcholine receptor, with implications for the binding of varenicline. Mol Pharmacol 84:201-207.

Wang DX, Booth H, Lerner-Marmarosh N, Osdene TS, and Abood LG (1998) Structure-activity relationships for nicotine analogs comparing competition for [^{3}H]nicotine binding and psychotropic potency. Drug Dev Res 45: 10-16.

Wildeboer K (2005) Structure activity relationships of nicotine analogs and *Erythrina* alkaloids on the alpha4beta2 nicotinic acetylcholine receptor. Ph.D. Dissertation, University of Florida, pp.1-107.

Wu J., and Lukas RJ (2011) Naturally-expressed nicotinic receptor subtypes. Biochem Pharmacol 82:800-807.

Xiu X, Puskar NL, Shanata JAP, Lester HA, and Dougherty DA (2009) Nicotine binding to brain receptors requires a strong cation-π interaction. Nature 458:534-538.

Zhao L, Kuo Y-P, George AA, Peng J-H, Purandare, MS, Schroeder KM, Lukas RJ, and Wu J (2003) Functional properties of homomeric, human α7-nicotinic acetylcholine receptors heterologously expressed in the SH-EP1 human epithelial cell line. J Pharmacol Exper Ther 305:1132-1141.

Zouridakis M, Giastas P, Zarkadas E, Chroni-Tzartou, Bregestovski P, and Tzartos SJ (2014) Crystal structures of free and antagonist-bound states of human α9 nicotinic receptor extracellular domain. Nat Struct Mol Biol 21:976-80.

Molecular Pharmacology Fast Forward. Published on May 30, 2020 as DOI: 10.1124/mol.119.118786
This article has not been copyedited and formatted. The final version may differ from this version.

ACKNOWLEDGEMENTS

We thank Dr. Steve Hagan for use of his spectropolarimeter, Drs. C-K. Tu for assistance with computer analysis associated with the pK_a determinations, Claire Stokes for advice on *Xenopus* oocyte preparation and mRNA injection, and Roger Papke for assistance with Pclamp software. Portions of this investigation were part of the Ph.D. dissertation of Kristin W. Andrud (Wildeboer, 2005). This research was funded by a Florida Biomedical Research Program grant (BM013, PI: WR Kem).

Molecular Pharmacology Fast Forward. Published on May 30, 2020 as DOI: 10.1124/mol.119.118786
This article has not been copyedited and formatted. The final version may differ from this version.

Table 1. Functional properties of nicotine analogs acting on human α7 receptors expressed in *Xenopus* oocytes. Peak current (PC) and net charge (NC) estimates were obtained from each response. Mean estimates ± one sample standard deviation of the maximum current response (I_{max}) and potency (EC_{50}) are given. (n = the number of oocytes used)

	EC_{50} (μM)			I_{max} (% of ACh Response)			
Compound	Peak Current	Net Charge	PC/NC Ratio	Peak Current	Net Charge	PC/NC Ratio	n
Nic (N)	65.3±20	21.2±7.4	3.1	91.5±10	85.4±20	1.1	7
1'-MeN	51.4±11	16.7±4.5	3.1	109±11	90.3±9.6	1.2	5
1'-EtNorN	85.2±22	30.7±12	2.8	54.1±15***	55.9±10	1.0	9
2'-MeN	9.65±4.0***	3.15±0.70***	3.1	82.4±6.9	72.0±7.2	1.1	5
3'Trans-MeN	46.7±14	13.8±8.3	3.4	115±25	64.6±11	1.8	5
3'Cis-MeN	171±45*^{ttt}	68.1±42*	2.5	92.5±29	62.6±8.5	1.5	5
4'Trans-MeN	246±58***	113±32***	2.2	16.4±4.6***	27.3±4.6***	0.60	4
4'Cis-MeN	277±32***	186±120**	1.5	1.81±0.80***	8.08±5.6***	0.20	4
5'Trans-MeN	134±53*	39.3±15	3.4	67.4±13	54.8±6.6*	1.2	7
5'Cis-MeN	1010±860***^{tt}	479±110***^{ttt}	2.1	4.42±2.0***^{ttt}	14.8±7.2***^{ttt}	0.3	4

*$p < 0.05$, **$p < 0.01$, ***$p < 0.001$ Comparison with nicotine (These p values were obtained from one way ANOVA of log transformed data with Dunnett's multiple comparison post-test.)
$^{t}p < 0.05$, $^{tt}p < 0.01$, $^{ttt}p < 0.001$ Comparison of cis- and trans-enantiomers; these p values were obtained from a two-tailed t test, and thus are not corrected for multiple comparisons.

Molecular Pharmacology Fast Forward. Published on May 30, 2020 as DOI: 10.1124/mol.119.118786
This article has not been copyedited and formatted. The final version may differ from this version.

Table 2. Nicotine analog binding to mammalian α7 nAChRs as measured by displacement of [^{125}I]-α-BTX specific binding. Mean K_i estimates ± one sample standard deviation are given. (n = the number of experiments)

Compound	Rat Brain Receptor			Human Receptor (SH-EP1 Cell)		
	K_i (nM)	-Hill Slope	n	K_i (nM)	-Hill Slope	n
Nic (N)	808±85	3.0	6	551±140	1.1	5
1'-MeN	817±74	2.5	3	917±200***	1.5	4
1'-EtNorN	2,620±340***	2.3	4	2,370±32***	1.2	4
2'-MeN	181±34***	2.9	7	144±24***	1.2	4
3'Trans-MeN	752±120	2.4	4	756±54*	1.2	4
3'Cis-MeN	3,120±500***^{ttt}	3.1	4	4,780±12***^{ttt}	1.0	3
4'Trans-MeN	3,910±30***	2.4	4	6,850±630***	1.5	5
4'Cis-MeN	2,930±58***^{ttt}	2.4	4	3,300±16***^{ttt}	1.3	2
5'Trans-MeN	2,130±76***	1.5	3	1,970±420***	1.1	4
5'Cis-MeN	34,800±2,600***^{ttt}	2.0	4	22,500±2,600***^{ttt}	1.1	4

*$p < 0.05$, **$p < 0.01$, ***$p < 0.001$ Comparison with nicotine (These p values were obtained from one way ANOVA of log transformed data with Dunnett's multiple comparison post-test.)

$^{t}p < 0.05$, $^{tt}p < 0.01$, $^{ttt}p < 0.001$ Comparison of cis- and trans-enantiomers; these p values were obtained from a two-tailed t test, and thus are not corrected for multiple comparisons.

Molecular Pharmacology Fast Forward. Published on May 30, 2020 as DOI: 10.1124/mol.119.118786
This article has not been copyedited and formatted. The final version may differ from this version.

Table 3. Functional properties of nicotine analogs acting on human α4β2 receptors expressed in *Xenopus* oocytes. Mean estimates ± one sample standard deviation are given. (n = the number of oocytes used).

Compound	EC_{50} (μM)	I_{max} (% ACh Response)	n
Nic (N)	0.430±0.33	93.8±14	11
1'-Et-NorN	3.65±2.1***	26.8±10***	6
1'-MeN	1.38±0.45***	22.5±5.4***	5
2'-MeN	0.738±0.089	83.4±14	5
3'Trans-MeN	0.74±0.42	52.9±14***	5
3'Cis-MeN	3.83±1.2$^{***\ ttt}$	51.4±5.4***	5
4'Trans-MeN	0.254±0.04	55.7±27***	5
4'Cis-MeN	0.285±0.14	32.7±14***	4
5'Trans-MeN	>300***	<1***	4
5'Cis-MeN	>300***	<1***	4

$^{*}p < 0.05$, $^{**}p < 0.01$, $^{***}p < 0.001$ Comparison with nicotine (These p values were obtained from one way ANOVA of log transformed data with Dunnett's multiple comparison post-test.)

$^{t}p < 0.05$, $^{tt}p < 0.01$, $^{ttt}p < 0.001$ Comparison of cis- and trans-enantiomers; these p values were obtained from a two-tailed t test, and thus are not corrected for multiple comparisons.

Molecular Pharmacology Fast Forward. Published on May 30, 2020 as DOI: 10.1124/mol.119.118786
This article has not been copyedited and formatted. The final version may differ from this version.

Table 4. Nicotine analog binding to mammalian α4β2 nAChRs measured by displacement of [^{3}H]-cytisine specific binding. Mean K_i estimates ± one sample standard deviation are given. (n = the number of experiments)

	Rat Brain Receptor			Human Receptor (tsA201)		
Compound	K_i (nM)	-Hill Slope	n	K_i (nM)	-Hill Slope	n
Nic (N)	3.26±0.78	0.85	6	3.53±0.92	0.89	5
1'-MeN	147±18***	0.84	4	158±79**	0.87	8
1'-EtNorN	83.1±20***	0.80	5	91.6±22***	1.0	4
2'-MeN	3.13±1.5	1.3	4	6.65±1.7**	1.4	4
3'Trans-MeN	73.7±13*** ^{ttt}	0.94	4	161±37*** ^{ttt}	0.92	6
3'Cis-MeN	770±71 ***	1.0	6	1,380±400***	1.2	4
4'Trans-MeN	14.9±5.1***	1.0	6	14.0±6.9**	1.1	6
4'Cis-MeN	24.4±7.1*** ^{t}	1.1	6	32.6±16** ^{t}	1.8	3
5'Trans-MeN	150±26***	1.0	4	219±76 ***	1.0	4
5'Cis-MeN	10600±1620**^{ttt}	0.87	5	8330±1030*** ^{ttt}	0.97	6

*$p < 0.05$, **$p < 0.01$, ***$p < 0.001$ Comparison with nicotine (These p values were obtained from one way ANOVA of log transformed data with Dunnett's multiple comparison post-test.)

$^{t}p < 0.05$, $^{tt}p < 0.01$, $^{ttt}p < 0.001$ Comparison of cis- and trans-enantiomers; these p values were obtained from a two-tailed t test, and thus are not corrected for multiple comparisons.

Molecular Pharmacology Fast Forward. Published on May 30, 2020 as DOI: 10.1124/mol.119.118786
This article has not been copyedited and formatted. The final version may differ from this version.

Table 5. Nicotine analog free energies of binding to the two human nAChRs compared with free energies of binding predicted from AChBP crystal structure docking. The number within parentheses is the % increase in ΔG of the analog relative to the ΔG for nicotine; a plus value represents a reduced affinity of the analog for the receptor relative to nicotine.

Compound	Human Receptor		AChBP	
	α7(SH-EP1 Cell)	α4β2 (tsA201 Cell)	Aplysia α7	Lymnaea
	-ΔG (Kcal/mol)		Predicted -ΔG (Kcal/mol)	
Nic (N)	8.88 (0%)[1]	10.77 (0%)[1]	8.882	8.883
1'-MeN	8.58 (+3%)	8.66 (+20%)	---	---
1'-EtNorN	7.99 (+10%)	8.96 (+17%)	---	---
2'-MeN	9.72 (-9%)	10.42 (+3%)	9.21	6.09
3'Trans-MeN	8.70 (+2%)	8.66 (+20%)	7.98	7.56
3'Cis-MeN	7.56 (+15%)	7.47 (+31%)	1.22	4.5
4'Trans-MeN	7.34 (+14%)	10.00 (+7%)	8.04	6.36
4'Cis-MeN	7.79 (+12)	9.54 (+11%)	6.3	5.01
5'Trans-MeN	8.11 (+9%)	8.48 (+21%)	8.37	7.16
5'Cis-MeN	6.60 (+26%)	6.47 (+40%)	8.33	3.66

[1] %ΔG change relative to ΔG for nicotine

[2] Predicted nicotine -ΔG= 34.1 Kcal/mol; normalized to 8.88

[3] Predicted nicotine -ΔG= 37.5 Kcal/mol; normalized to 8.88

Molecular Pharmacology Fast Forward. Published on May 30, 2020 as DOI: 10.1124/mol.119.118786
This article has not been copyedited and formatted. The final version may differ from this version.

Molecular Pharmacology Fast Forward. Published on May 30, 2020 as DOI: 10.1124/mol.119.118786
This article has not been copyedited and formatted. The final version may differ from this version.

Table 6. Radioligand binding affinities of six additional methylnicotine analogs for rat brain α4β2 and α7 receptors. Mean K_i estimates ± one sample standard deviation are given. (n = the number of experiments). The p values were obtained from a two-tailed t test comparing the two enantiomers, and thus are not corrected for multiple comparisons.

Compound	α4β2 Receptor			α7 Receptor		
	K_i (nM)	-Hill Slope	n	K_i (nM)	-Hill Slope	n
A84543[1]	3.44±0.40			340±50		
5'Trans-MeA84543	18.5±17^{tt}	1.0	4	603^{ttt}±170	1.9	5
5'Cis-MeA84543	201±26	1.0	3	2,140±830	1.8	5
5'Trans-Me(R)N	480±140^{t}	1.1	3	3920±2300	2.9	2
5'Cis-Me(R)N	204±89	1.0	5	426	2.8	1
3'Trans-Me(R)N	553±140^{ttt}	1.1	4	6720±710^{tt}	3.6	3
3'Cis-Me(R)N	4340±1400	1.1	4	22000±3600	1.7	3

$^{t}p < 0.05$, $^{tt}p < 0.01$, $^{ttt}p < 0.001$ Comparison of cis- and trans-enantiomers (These p values were obtained from a two-tailed t test.)

[1]A84543 K_i ±SEM binding data of Ogunjirin et al. (2015); Abreo et al (1996) reported K_i's of 0.15 nM and 1 nM for A84543 and nicotine, respectively, at rat brain α4β2 receptors

Molecular Pharmacology Fast Forward. Published on May 30, 2020 as DOI: 10.1124/mol.119.118786
This article has not been copyedited and formatted. The final version may differ from this version.

FIGURE LEGENDS

Figure 1. Structure and IUPAC nomenclature for (S)nicotine and A84543 monocations. The striated bond between the two rings indicates that the pyridyl substituent is situated below the pyrrolidinium ring, in the S-configuration.

Figure 2. *Xenopus* concentration-response curves for nicotine and the methylnicotines on human α7 (Left) and α4β2 (Right) nAChRs. Peak current responses were recorded by the two electrode voltage-clamp method described in Materials and Methods. Net charge EC_{50} and I_{max} values were also estimated from the same oocytes, and data obtained from both methods are summarized in Tables 1 and 3. The error bars indicate ±1 SEM. n=number of oocytes tested at a particular concentration. The complete concentration-response curves for nicotine and ACh, including numbers of oocytes tested at each concentration, are found in Supplement Figures 1S and 2S.

Figure 3. Correlations between *Xenopus* oocyte functional and cultured cell receptor binding data. I_{max} and EC_{50} estimates were determined from human α7 receptors expressed in *Xenopus* oocytes using the net charge method, while K_is were determined by [^{125}I]-BTX displacement using SH-EP1 cell membranes expressing human α7 receptors (A,B) , EC_{50}s from human α4β2 receptors expressed in oocytes and K_is from tsA201 cell membranes (C,D) (**A)**. Nicotine analog correlation between binding K_i from SH-EP1 cells and EC_{50} from α7 receptor *Xenopus* oocytes; (**B**) Nicotine analog correlation between α7 receptor net charge EC_{50} and I_{max} for each compound; **(C)** Nicotine analog correlation between and α4β2 receptor K_is (tsA201

Molecular Pharmacology Fast Forward. Published on May 30, 2020 as DOI: 10.1124/mol.119.118786
This article has not been copyedited and formatted. The final version may differ from this version.

cells) and EC_{50}s (oocytes); and (**D**) Nicotine analog correlation between human α4β2 receptor EC_{50} and I_{max}.

Figure 4. Concentration-response curves for 5'trans-methylA84543 stimulation of human α4β2 and α7 nAChRs expressed in *Xenopus* oocytes. The error bars indicate ±one SEM. (The 5'cis-methylA84543 enantiomer was much less active: at 30 μM the peak α7 response was approximately 10% of the 1 mM ACh response and the α4β2 response was ~0 % of the 100 μM ACh response).

Molecular Pharmacology Fast Forward. Published on May 30, 2020 as DOI: 10.1124/mol.119.118786
This article has not been copyedited and formatted. The final version may differ from this version.

Fig. 1

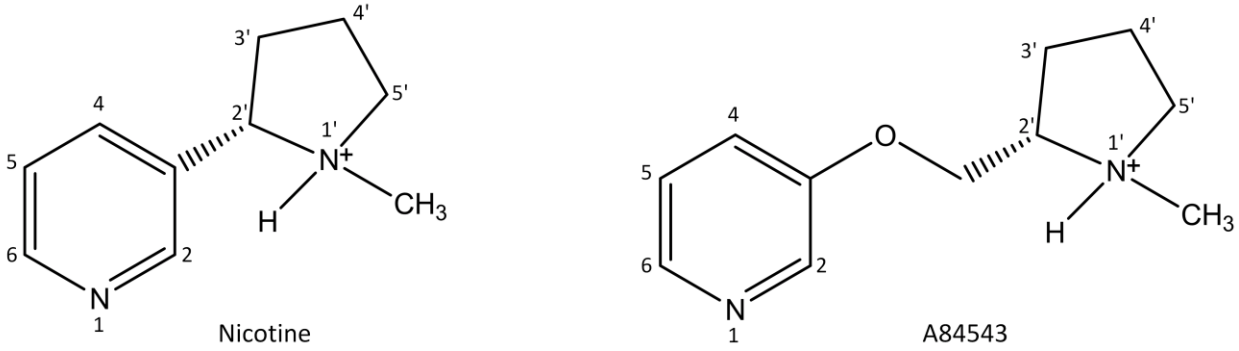

Molecular Pharmacology Fast Forward. Published on May 30, 2020 as DOI: 10.1124/mol.119.118786
This article has not been copyedited and formatted. The final version may differ from this version.

Fig. 2

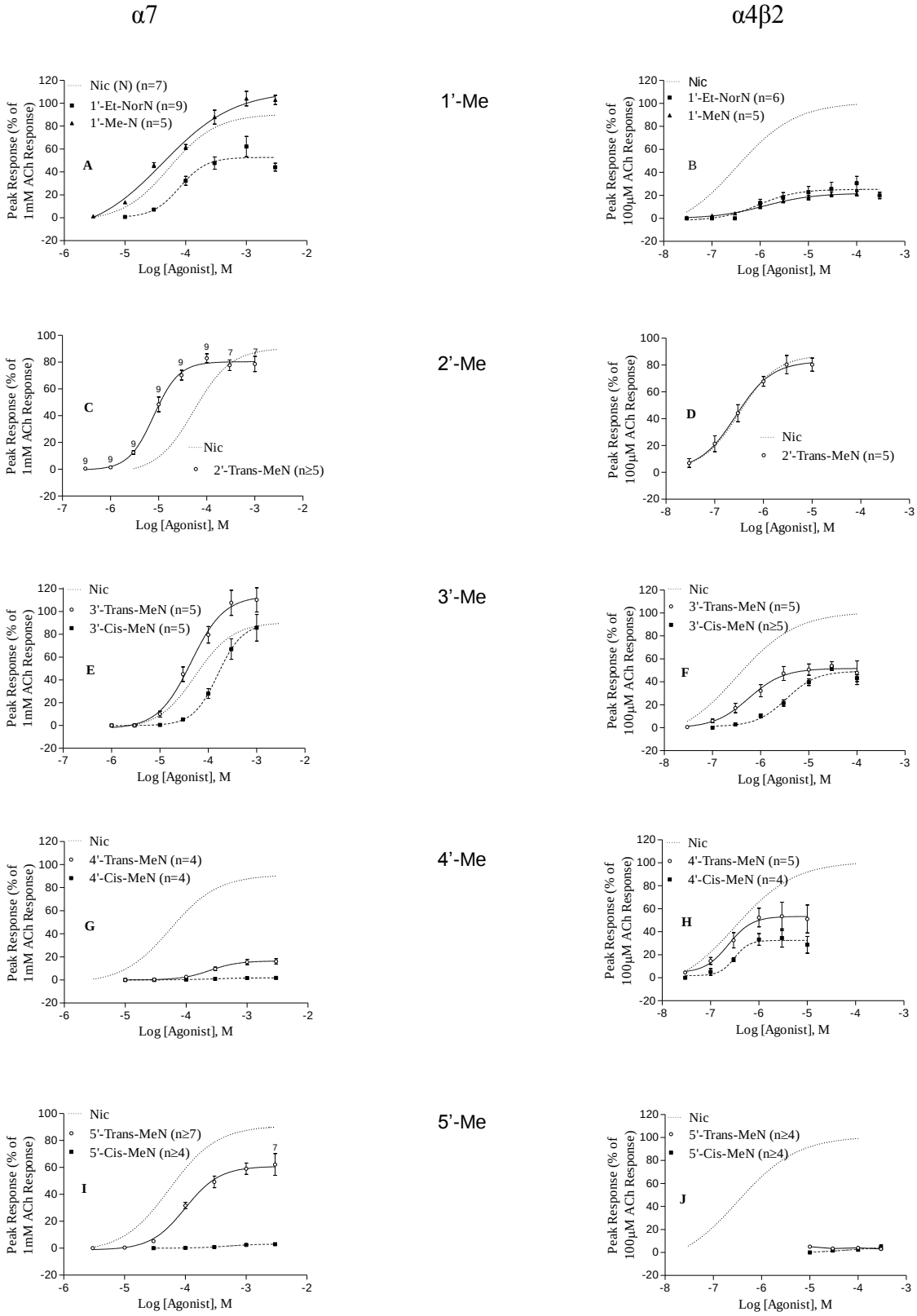

Molecular Pharmacology Fast Forward. Published on May 30, 2020 as DOI: 10.1124/mol.119.118786
This article has not been copyedited and formatted. The final version may differ from this version.

Fig.3

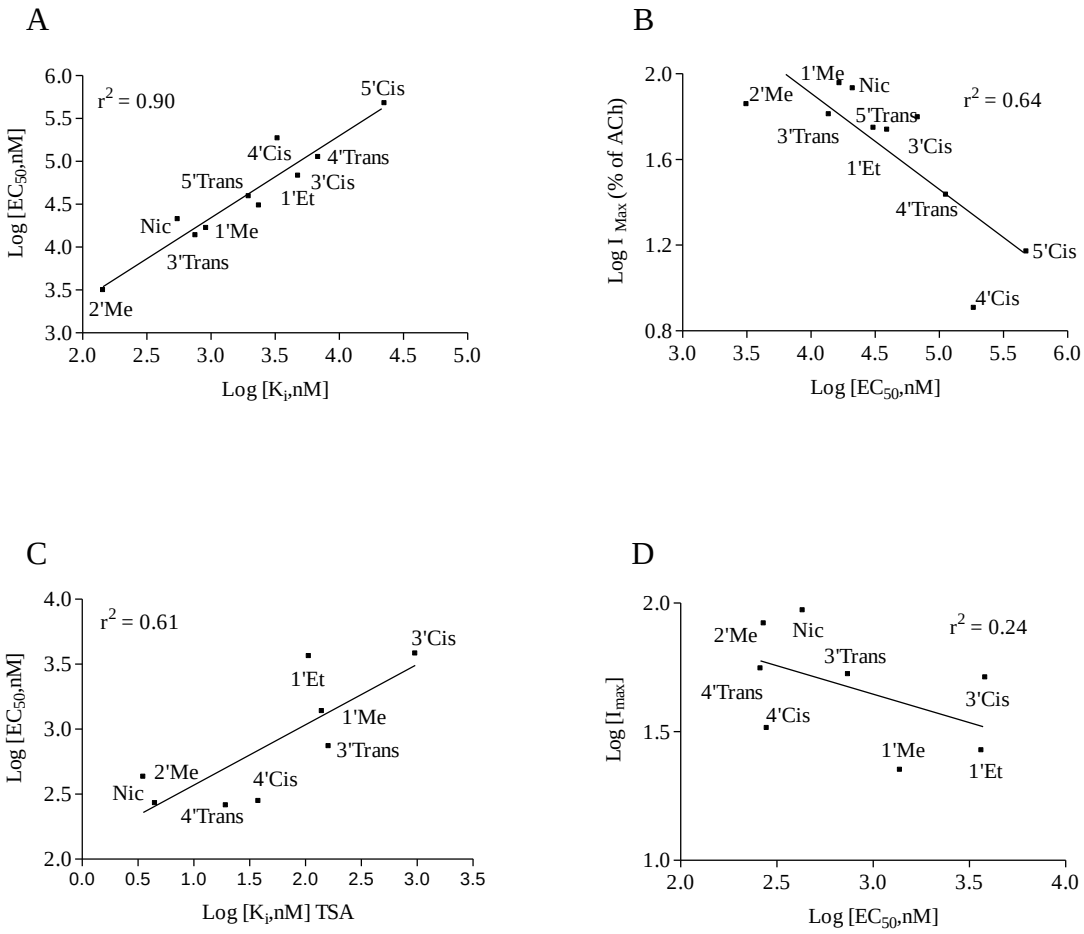

Molecular Pharmacology Fast Forward. Published on May 30, 2020 as DOI: 10.1124/mol.119.118786
This article has not been copyedited and formatted. The final version may differ from this version.

Fig. 4

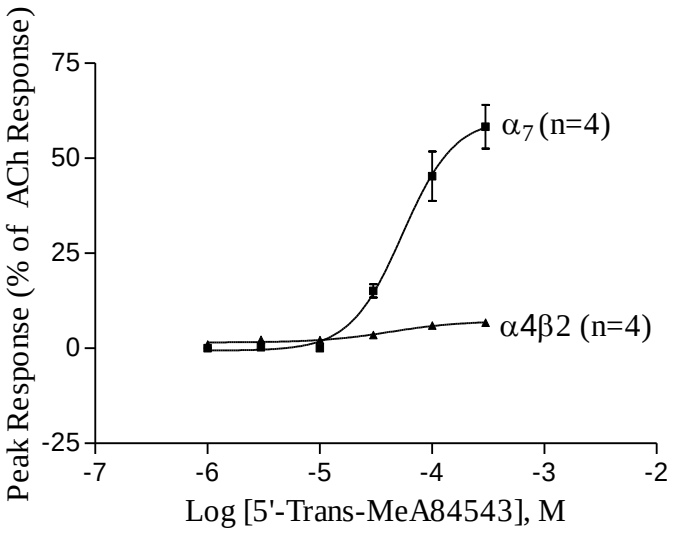

Authorship Contributions

Participated in research design: Xing, Andrud, Slavo, Jahn, Corsino, Lindstrom, and Kem

Conducted experiments: Xing, Andrud, Cho, Habibi, Ziang, Slavo, Jahn, Corsino and Kem

Contributed new reagents or analytic tools: Lukas, Lindstrom and Slavo

Performed data analysis: Xing, Andrud, Slavo, Jahn, Corsino, Cho, Habibi, Ziang, Lindstrom, and Kem

Wrote or contributed to the writing of the manuscript: Kem, Xing, Jahn, and Slavo, Ziang